JOHNSON, C. K. (1976). *ORTEP*II. Report ORNL-5138. Oak Ridge National Laboratory, Tennessee, USA.
KIRMSE, W., VON BÜLOW, B. & SCHEPP, H. (1966). *Justus Liebigs Ann. Chem.* **691**, 41–49.
MEIJERE, A. DE, SCHALLNER, O. & WEITEMEYER, C. (1973). *Tetrahedron Lett.* **36**, 3483–3486.
NES, G. J. H. VAN & VAN BOLHUIS, F. (1978). *J. Appl. Cryst.* **11**, 206–207.
NIJVELDT, D. & VOS, A. (1988*a*). *Acta Cryst.* B**44**, 289–296.
NIJVELDT, D. & VOS, A. (1988*b*). *Acta Cryst.* B**44**, 296–307.
REES, B. (1976). *Acta Cryst.* A**32**, 483–488.
STEWART, R. F., BENTLEY, J. & GOODMAN, B. (1975). *J. Chem. Phys.* **63**, 3786–3793.
STEWART, R. F. & SPACKMAN, M. A. (1981). *VALRAY Users Manual.* Preliminary Draft. Department of Chemistry, Carnegie-Mellon Univ., Pittsburgh, PA, USA.
TRÆTTEBERG, M. (1983). Private communication.
WAL, R. VAN DER (1982). PhD Thesis. Univ. of Groningen, The Netherlands.
WILSON, A. J. C. (1976). *Acta Cryst.* A**32**, 781–783.

Acta Cryst. (1988). B**44**, 289–296

Single-Crystal X-ray Geometries and Electron Density Distributions of Cyclopropane, Bicyclopropyl and Vinylcyclopropane. II. Multipole Refinements and Dynamic Electron Density Distributions

BY DICK NIJVELDT AND AAFJE VOS

Laboratory of Chemical Physics, University of Groningen, Nijenborgh 16, 9747 *AG Groningen, The Netherlands*

(*Received* 21 *November* 1986; *accepted* 9 *December* 1987)

Abstract

Multipole refinements have been carried out with the program *VALRAY* to obtain the most accurate models for the geometry and electron density description. During the ultimate multipole refinement on $|F|$, (i) independent reflections weighted with the reflection multiplicity were taken, (ii) extinction corrections were included for bicyclopropyl (BCP) and vinylcyclopropane (VCP), (iii) all available types of multipoles were used for C and H, *viz* up to hexadecapole level, and (iv) the form of the single exponential radial distribution functions for octopoles on C was varied. Final residuals are for cyclopropane (CP) C_3H_6: $R(F) = 0{\cdot}0211$, $R_w(F) = 0{\cdot}0198$; for BCP, C_6H_{10}: $R(F) = 0{\cdot}0210$, $R_w(F) = 0{\cdot}0194$; and for VCP, C_5H_8: $R(F) = 0{\cdot}0159$, $R_w(F) = 0{\cdot}0140$. Pronounced features in the dynamic filtered deformation density distributions are the bent bond character in the plane of the ring and the non-cylindrical distribution around the double bond in VCP.

1. Introduction

A refinement in which account is taken of the nonspherical density distribution of atoms in molecules will render a more realistic model than does a conventional 'spherical-atom' refinement. During these multipole refinements the atomic density functions are taken as rigid and centred on the nuclei. In the present refinements the thermal vibrations are assumed to be harmonic. Experimental $|F|$'s have not been corrected for thermal diffuse scattering. Simple functions have been taken for the radial distributions of the multipoles, because adjustment of complicated functions showing sharp high-resolution features to the observed density is hampered by thermal smearing and limited resolution [van der Wal (1982); refinements on hypothetical SiO having quantum theoretical density affected by thermal smearing and limited resolution].

The electron density distribution is given with respect to the independent atom model (IAM), as a reference. This IAM is chosen as a superposition of the spherically averaged electron densities of atoms p in the

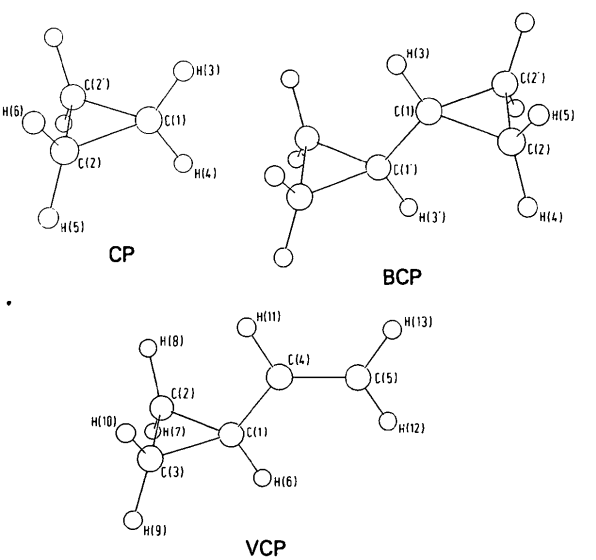

Fig. 1. Atomic numbering in CP, BCP and VCP. Numbers which are related by crystallographic symmetry (paper I, §6), are given as p and p'.

0108-7681/88/030289-08$03.00

ground state. Corresponding nuclei in the IAM and in the real crystal have the same positions $\mathbf{r}_p$ and thermal tensors $\mathbf{U}_p$. The difference density obtained in this way is generally called the deformation density:

$$\Delta\rho(\mathbf{r}) = \rho(\text{crystal};\mathbf{r})\text{-}\rho(\text{IAM},\mathbf{r}_p,\mathbf{U}_p;\mathbf{r}). \quad (1)$$

In the present study, $\mathbf{r}_p$ and $\mathbf{U}_p$ are taken from the ultimate multipole refinements. Molecular formulae and atomic numbering are given in Fig. 1.

2. Multipole refinements

2.1. *Multipole functions applied*

The program *VALRAY* (Stewart & Spackman, 1981, and literature quoted therein) has been used for the multipole refinements. The five available types of multipole function are indicated by l, which ranges from 0 to 4: monopole, dipole, quadrupole, octopole and hexadecapole level. Each level corresponds to one radial distribution function ($i = 1$), except for the monopole level where two types of function ($i = 1$ or 2) will be distinguished. In the adopted multipole model the density of each pseudoatom p is described by the independent atom (IA) density ($i = 1, l = 0, m = 0$) plus the sum of the deformation contributions ($i = 2, l = 0, m = 0$ and $i = 1, l \geq 1, |m| \leq l$). The total model electron density in the unit cell can be written, on a relative scale, as

$$\rho(\text{model};\mathbf{r}) = \text{Sc}\,\rho(\text{IAM};\mathbf{r}) + \text{Sc DEF(model};\mathbf{r}), \quad (2)$$

where

$$\text{Sc}\,\rho(\text{IAM};\mathbf{r}) = \sum_p [\text{Pop}_p(1,0,0)\rho_p(1,0,R_p)]$$

and

$$\text{Sc DEF(model};\mathbf{r}) = \sum_p [\text{Pop}_p(2,0,0)\rho_p(2,0,R_p) + \sum_{l=1}^{l_{\max}} \sum_{m=0}^{l} \text{Pop}(1,l,m\pm)\rho_p(1,l,R_p)Y_{l,m\pm}(\Theta_p,\Phi_p)].$$

The scale factor Sc is estimated as

$$\text{Sc} = \sum_p \sum_{i=1}^{2} \text{Pop}_p(i,0,0)/F(000),$$

where summation is over all atoms p in the unit cell, which contains $F(000)$ electrons. $\text{Pop}_p(i,l,m\pm)$ gives for atom p and Tesseral harmonic $Y_{lm\pm}$ the population of the ith radial distribution function $\rho_p(i,l,R_p)$. The Tesseral harmonics $Y_{lm\pm}$ define the shape of the multipole function. $\mathbf{R}_p = \mathbf{r}-\mathbf{r}_p$ is the vectorial distance from nucleus p at $\mathbf{r}_p$ and has in a chosen crystal related orthogonal reference frame **X**, **Y**, **Z**, angular components Θ_p, Φ_p.

All atoms of the same type have the same IA population Pop(1,0,0); the IA population of H is set to 1/6th of the C IA population. The C IA scattering factor has been derived from Clementi's (1965) analytical (^3P) wave function. The IA scattering factor for H corresponds with the contracted monopole function deduced from the density distribution of H_2 by Stewart, Bentley & Goodman (1975).

For the deformation functions two types of scattering factors, *A* and *S*, will be distinguished.

A type. Scattering factors deduced from single exponential or Slater-type functions (STF):

$$\rho_p(l,R_p) = (4\pi)^{-1}[\alpha^{n+l+3}/(n+l+2)!]R_p^n\exp(-\alpha R_p),$$

where α is a continuous variable which may be different for a different l. The discrete n's are restricted to $n \geq l$. α has been chosen as a refinable parameter for C octopoles, since these multipoles turned out to have the largest deformation populations. Fixed α values are taken equal to the standard molecular values; $\alpha_C = 6{\cdot}50$ and $\alpha_H = 4{\cdot}69$ Å^{-1} (Hehre, Stewart & Pople, 1969; Bentley & Stewart, 1976). The n's are chosen according to van Nes & van Bolhuis (1979); for C, $n(l = 1) = 2$, $n(l > 1) = l$, and for H, $n(l) = l$.

S type. Self-consistent field (SCF) scattering factors based upon the same SCF calculations as the corresponding IA values. Owing to their limited availability, they are supplemented by *A*-type scattering factors for $l \geq 3$ in refinements with $l_{\max} > 2$.

In addition to the standard multipole functions, the so-called *polarized hydrogens* are available, which consist of one monopole and one dipole function with equal populations. The positive lobe of the deformation function is directed towards the connected atom. Fixed radial distribution functions are applied which correspond with the quantum theoretical H_2 density mentioned above.

2.2. *Reference frame*

The orthogonal reference frame **X**, **Y**, **Z** of each compound is chosen in such a manner that restraints on the angular part of the multipoles can be formulated in an easy way. The restraints are imposed by crystallographic symmetry (see §6 of Nijveldt & Vos, 1988*a*; hereinafter referred to as paper I) and/or by adopted local symmetry. In bicyclopropyl (BCP) the crystallographic point-group symmetry $2/m$ for the molecule fixes one direction of the reference frame; **X** is taken parallel to the twofold axis and **Y** perpendicular to the ring. In cyclopropane (CP) and vinylcyclopropane (VCP) local pseudo-symmetry planes (**X**,**Y**) have been adopted. In CP the pseudo-symmetry plane coincides with the ring plane; **X** is taken parallel to C(2)–C(2′) (Fig. 1) and consequently perpendicular to the crystallographic mirror plane. In VCP the C(1)C(4)C(5) plane is taken as the (**X**,**Y**) plane, with **X** parallel to C(4)–C(5).

2.3. *Refinement of the multipole model*

In the least-squares refinement the function minimized reads

$$Q = \sum_{\mathbf{H}} w(\mathbf{H}) \mid F_o(\mathbf{H}) - F_c(\mathrm{rel};\mathbf{H}) \mid^2,$$

where summation **H** is over the independent reflections. Weights are $w(\mathbf{H}) = 0$ for $\mid F_o(\mathbf{H}) \mid \leq \kappa\sigma[F_o(\mathbf{H})]$ (paper I, § 7.1) and $w(\mathbf{H}) = m(\mathbf{H})$, reflection multiplicity, for $\mid F_o(\mathbf{H}) \mid > \kappa\sigma[F_o(\mathbf{H})]$ [paper I, § 4.2 and 7.1; $w(\mathbf{H}) = m(\mathbf{H})$ applied to independent reflections corresponds with uniform weights if all reflections are considered].

Residuals are defined as

$$R(F) = [\sum_{\mathbf{H}} \big| \mid F_o(\mathbf{H}) \mid - \mid F_c(\mathrm{rel};\mathbf{H}) \mid \big|][\sum_{\mathbf{H}} \mid F_o(\mathbf{H}) \mid]^{-1}$$

and

$$R_w(F) = \{[\sum_{\mathbf{H}} w(\mathbf{H}) \big| \mid F_o(\mathbf{H}) \mid - \mid F_c(\mathrm{rel};\mathbf{H}) \mid \big|^2] \times [\sum_{\mathbf{H}} w(\mathbf{H}) \mid F_o(\mathbf{H}) \mid^2]^{-1}\}^{1/2}.$$

An anisotropic temperature factor

$$T(\mathbf{H}) = \exp[-2\pi^2(h^2a^{*2}U_{11} + k^2b^{*2}U_{22} + l^2c^{*2}U_{33} + 2hka^*b^*U_{12} + 2hla^*c^*U_{13} + 2klb^*c^*U_{23})]$$

is applied to C as well as to H atoms.

2.4. *Hydrogen atoms*

Because of the strong drop of the hydrogen scattering factor with increasing $(\sin\theta)/\lambda$, for each H atom large correlations are expected between (i) position and dipole deformation, (ii) thermal tensor **U** and quadrupole deformation, and (iii) monopole population and isotropic part of the temperature factor.

Correlation (i) has been avoided by constraining the H positions to the C positions. The direction of each C—H bond is obtained prior to each multipole refinement from a so-called polarized H refinement: an analogous refinement, but with H replaced by the polarized hydrogen of § 2.1 with adjustable position. The standard deviations σ(H—C—H) vary from 0·5° in BCP to 1·2° in CP. Subsequently, each H position is fixed along the C—H direction at

$$l_j(\mathrm{C{-}H}) = l_j(\mathrm{C{-}H;XR}) + \Delta, \qquad (3a)$$

where l_j(C—H;XR) is the length of the jth C—H bond obtained from the polarized H refinement and Δ is a correction derived from electron diffraction (ED) C—H lengths l(ED)'s. For each of the compounds Δ is taken the same for all C—H bonds since ED yields only average C—H distances (Table 1). To match l(ED) with the harmonic thermal motion description of the X-ray refinements, a librational shortening has been applied to l(ED). The correction Δ is given by

Table 1. *Average XR and ED bond lengths* (Å)

XR values have been taken from the UM refinements (§ 2.7). The XR C—H distances do not contain the correction Δ given by equation (3*b*).

	Type	⟨C—C⟩ ring	⟨C—H⟩	Reference
CP	XR	1·4991 (7)	1·029 (5)	
	ED	1·5096 (15)	1·089 (3)	(*a*)
BCP	XR	1·5050 (3)	1·061 (3)	
	ED	1·507 (3)	1·1034 (20)	(*b*)
VCP	XR	1·5090 (3)	1·046 (3)	
	ED	1·516 (3)	1·1043 (13)	(*c*)

References: (*a*) Bastiansen, Fritsch & Hedberg (1964); (*b*) Hagen, Hagen & Trætteberg (1972); (*c*) Trætteberg (1983).

$$\Delta = l(\mathrm{ED}) - \Delta(\mathrm{lib}) - \langle l_j(\mathrm{C{-}H;XR})\rangle, \qquad (3b)$$

in which the angle brackets indicate the average over all C—H lengths of the compound considered. Use of the same Δ for all C—H's of a compound is not unrealistic since for each of the compounds all l_j(C—H;XR) values turned out to be equal within experimental error. The libration correction Δ(lib) is taken the same for all three molecules. Its value of 0·020 Å contains a contribution of 0·014 Å from internal librations [deduced from Raman/IR study on CP by Levin & Pearce (1978) with the procedure of Keulen (1969)], and a contribution of 0·006 Å for external libration (estimated from average shortening of C—C ring bond lengths with respect to ED lengths, Table 1). For the ultimate multipole refinements the Δ's are 0·040 for CP, 0·022 for BCP and 0·038 Å for VCP.

To avoid correlation (ii) the H quadrupole deformation, which is expected to be small, has been set to zero. Correlation (iii) has been reduced by constraining the IA population of H to that of C. Moreover monopole deformation populations are taken the same for all H's.

Owing to the large correlations the adopted hydrogen model still gives a good representation of the total observed density distribution. In DEF(model;**r**) maps, however, the deformation around H will be affected by the assumptions made above.

2.5. *Summary of restraints and constraints*

All multipole refinements have been subjected to the following restraints or constraints.

1. $\mathrm{Pop}(1,0,0)[\mathrm{C}(p)] = \mathrm{Pop}(1,0,0)[\mathrm{C}]$, IA constraint, § 2.1.
2. $6\ \mathrm{Pop}(1,0,0)[\mathrm{H}] = \mathrm{Pop}(1,0,0)[\mathrm{C}]$, IA constraint, § 2.1.
3. $\mathrm{Pop}(2,0,0)[\mathrm{H}(p)] = \mathrm{Pop}(2,0,0)[\mathrm{H}]$, see § 2.4.
4. $\sum_p \mathrm{Pop}_p(2,0,0) = 0$, molecular neutrality constraint.
5. $l_j(\mathrm{C{-}H}) = l_j(\mathrm{C{-}H;XR}) + \Delta$, see § 2.4.

p ranges over all (relevant) atoms in the unit cell, and j refers to the individual C—H bonds.

In addition to these general constraints, restraints with respect to the following pseudo-symmetry elements are used for all CP and VCP refinements.

CP 6. Mirror plane coinciding with ring plane for multipole populations of individual C atoms.
7. Threefold symmetry relating monopole populations and octopole α's of the three ring C atoms.

VCP 6. Mirror plane coinciding with C(1)C(4)C(5) for multipole populations of C(1), C(4) and C(5), and for monopole populations and octopole α's of C(2) and C(3).

Finally, in §2.7 some additional 'pseudo-symmetry restraints' are introduced in cases where DEF(model; **r**) turned out to deviate from expected symmetry.

CP SYM: Symmetry imposed on C(2) multipole populations with respect to an assumed mirror plane perpendicular to the ring and bisecting the C(2) endocyclic angle.

VCP C=C: Octopole parameters of C(4) and C(5) restrained with respect to an assumed symmetry plane perpendicular to and through the centre of the double bond. Moreover $\alpha(l=3)[C(2)] = \alpha(l=3)[C(1)]$.

2.6. *Nomenclature*

The different refinements have been coded by the string 'Type' (l_C,l_H) 'Extra', with the following possible substitutions.

'Type': *A*; STF scattering factors for the deformation functions, §2.1.
S; SCF scattering factors for the deformation functions, §2.1.
l_C: 3 to 4; l_{max}, highest multipole level for C atoms.
l_H: 1 to 4; l_{max}, highest multipole level for H atoms.
'Extra': *E*; Application of extinction correction, §2.7.
*A*3; Adjustable $\alpha(l=3)$ for C, §2.1.
SYM; Pseudo-symmetry restraint, §2.5.
C=C; Pseudo-symmetry restraint, §2.5.

2.7. *Refinement procedure and ultimate multipole models*

Because of its centrosymmetric structure and relatively small thermal motion, BCP has been used to determine the refinement strategy with respect to scattering factors, octopole α's and extension of the multipole set.

Scattering factors. Corresponding *A*- and *S*-type refinements (§2.1) on BCP do not reveal significant differences for the parameters $\mathbf{r}_p$ and $\mathbf{U}_p$, or for the peaks in the residual and deformation density maps. The residual R_w, however, shows a small decrease when the refinement is changed from *A* to *S*. Examples are:

A(4,3): $R_w = 2{\cdot}41\%$ *S*(4,3): $R_w = 2{\cdot}37\%$
A(4,3)*E*: $R_w = 2{\cdot}00\%$ *S*(4,3)*E*: $R_w = 1{\cdot}98\%$.

It was decided to use *S*-type scattering factors for all refinements. The results of different *S* refinements on CP, BCP and VCP are listed in Table 2.

Extinction. Inspection of strong low-order reflections, after *S*(3,1) refinements on BCP and VCP, showed the tendency of $|F_o(\mathbf{H})|$ to be smaller than $|F_c(\text{rel};\mathbf{H})|$. For reflections with $|F_o(\mathbf{H})| > \frac{1}{2}|F_o|_{max}$ the mean difference $\langle |F_o(\mathbf{H})| - |F_c(\text{rel};\mathbf{H})| \rangle = \sum_{\mathbf{H}} m(\mathbf{H})[|F_o(\mathbf{H})| - |F_c(\text{rel};\mathbf{H})|]/\sum_{\mathbf{H}} m(\mathbf{H})$, is +0·05 (4) for CP, −0·65 (25) for BCP and −0·48 (20) for VCP. Therefore an extinction correction has not been applied to CP; trial refinements [Becker & Coppens (1974) formalism; type I; Lorentzian mosaic spread] gave extinction parameters with negative sign. Table 2 shows a significant decrease of R_w when the correction is introduced for BCP and VCP. The correction increases Sc, $\langle U_{eq} \rangle_C$ and the density maxima on the C—C bonds in DEF(model;**r**).

Radial distribution of octopole functions. Since the C octopole deformations are by far the largest, the influence of refinement of $\alpha(C;l=3)$ has been studied. Addition of the two variable α's to the *S*(3,1)*E* refinement on BCP produced a significant drop in R_w from 0·94 to 0·82 for low-order reflections up to $(\sin\theta)/\lambda = 0{\cdot}65$ Å^{-1} [R_w factor ratio of 1·02 at 0·5% significance level (Hamilton, 1965) is smaller than the observed ratio of 1·15]. Consequently the *A*3 refinement has also been applied to CP and VCP. In the UM models described below the average deviations of $\alpha(l=3)$ from the standard molecular value of 6·50 Å^{-1} are −0·81 (23) for CP, −0·45 (11) for BCP and −0·96 (8) Å^{-1} for VCP. The decrease in α changes the position of the octopole maximum, found at $R_{max} = n/\alpha = 3/\alpha = 0{\cdot}461$ Å for $\alpha = 6{\cdot}50$ Å^{-1}, to $R_{max} = 0{\cdot}527$ (11) for CP, 0·496 (5) for BCP, and 0·542 (4) Å for VCP.

Extension of the multipole set. Refinements for the BCP reflections up to $(\sin\theta)/\lambda = 0{\cdot}65$ Å^{-1} with IA parameters Pop(1,0,0), $\mathbf{r}_p$ and $\mathbf{U}_p$ fixed at *S*(3,1)*E*,*A*3 full-angle values, give a significant decrease in R_w from 0·82% for *S*(3,1)*E*,*A*3 to 0·57% for *S*(4,4)*E*,*A*3 [R_w ratio of 1·44 is clearly larger than R_w ratio of 1·19 at 0·5% significance level (Hamilton, 1965)]. Consequently hexadecapole functions have also been introduced for CP and VCP; experimental and theoretical R_w factor ratios are given in Table 3.

Additional pseudo-symmetry. The CP ring plane *S*(4,4) DEF(model;**r**) density at C(2) shows strong deviations from the expected pseudo-symmetry with respect to the plane perpendicular to the ring and bisecting the C(2) endocyclic angle (Fig. 2*a*). For VCP the *S*(4,4)*E*,*A*3 DEF(model;**r**) map reveals unexpected

Table 2. *Data concerning the progress of the multipole refinements*

Column headings are: N_v: number of refined parameters; Ext: maximum reduction in $|F_c(\mathbf{H})|$ due to extinction correction, for BCP in reflection 200 and for VCP in $11\bar{1}$; $U_{eq} = \frac{1}{3}\sum_i\sum_j U_{ij}a_i^*a_j^*\mathbf{a}_i.\mathbf{a}_j$; DEF_{max}: maximum of the deformation density DEF (model; **r**) at a C–C bond. The units are: R (%), Ext (%), U_{eq} (10^{-5} Å^2) and DEF_{max} (10^{-2} e Å^{-3}).

Refinement	N_v	Sc	R	R_w	Ext	$\langle U_{eq}\rangle_C$	DEF_{max} Adjacent		Distal	Central	Double
CP							C(1)–C(2)	C(2)–C(2′)			
S(3,1)	62	0·995 (11)	2·35	2·06	—	2585	25	21			
S(4,4)	120	0·993 (16)	2·13	1·98	—	2578	28	22			
S(3,1)*A*3,SYM	58	0·992 (13)	2·28	2·04	—	2576	23	20			
S(4,4)*A*3,SYM	114	0·992 (14)	2·11	1·98	—	2573	27	24			
BCP							C(1)–C(2)				
S(3,1)	67	1·0057 (12)	2·69	2·49	—	1953	20		17	35	
S(3,1)*E*	68	1·018 (4)	2·30	2·06	10·1	1981	25		24	37	
S(3,1)*E*,*A*3	70	1·015 (4)	2·24	2·02	9·9	1976	24		24	35	
S(4,4)*E*,*A*3	125	1·015 (5)	2·10	1·94	9·9	1974	29		25	37	
VCP							C(1)–C(2)	C(1)–C(3)			
S(3,1)	175	0·9980 (14)	2·27	2·18	—	2029	19	18	21	41	59
S(3,1)*E*	176	1·0071 (18)	1·76	1·50	8·9	2051	24	24	24	45	60
S(3,1)*E*,*A*3	180	1·0035 (17)	1·67	1·44	8·8	2043	24	25	23	43	57
S(4,4)*E*,*A*3	309	1·0023 (24)	1·58	1·40	8·9	2040	29	29	28	44	57
S(3,1)*E*,*A*3,C=C	174	1·0036 (17)	1·69	1·44	8·8	2043	24	25	24	42	57
S(4,4)*E*,*A*3,C=C	305	1·0025 (23)	1·59	1·40	8·9	2040	29	29	28	45	57

Table 3. *R_w factor ratio's of comparable refinements with* (3,1) *and* (4,4) *multipole sets*

The data are restricted to $(\sin\theta)/\lambda < 0{\cdot}65$ Å^{-1}. Carbon IA values are fixed to the FA values of the (3,1)-type refinements.

Compound	Refinements (3,1) set	Refinements (4,4) set	$R_w(3,1)/R_w(4,4)$	*R*-factor ratio at 0·5% level
CP	*S*(3,1)*A*3,SYM	*S*(4,4)*A*3,SYM	0·54/0·39 = 1·38	1·38
BCP	*S*(3,1)*E*,*A*3	*S*(4,4)*E*,*A*3	0·82/0·57 = 1·44	1·19
VCP	*S*(3,1)*E*,*A*3,C=C	*S*(4,4)*E*,*A*3,C=C	0·48/0·32 = 1·50	1·24

shifts (≈0·1 Å) of the density maxima on C(1)–C(4) and C(4)–C(5) from their bond centres, towards C(1) and C(5) respectively (Fig. 2*b*). These shifts increase to 0·25 Å if the **U** tensors are set to zero in DEF(model;**r**). To check whether the unexpected asymmetries are significant the SYM,*A*3 restraint has been adopted for CP and the C=C restraint for VCP (§2.5). Both restraints can be considered as an improvement of the model since the decrease in the number of parameters increases neither R_w nor the integrated absolute residual density in the regions considered.

Ultimate multipole models. The ultimate multipole (UM) models are the result of the final refinements of Table 2.* Geometrical and thermal parameters and static densities are given and discussed by Nijveldt & Vos (1988*b*; hereinafter referred to as paper III). The estimated σ's in the C–C bond distances are small and increase in order 3 (BCP) < 4 (VCP) < 8 × 10^{-4} Å (CP). This sequence clearly demonstrates the influence

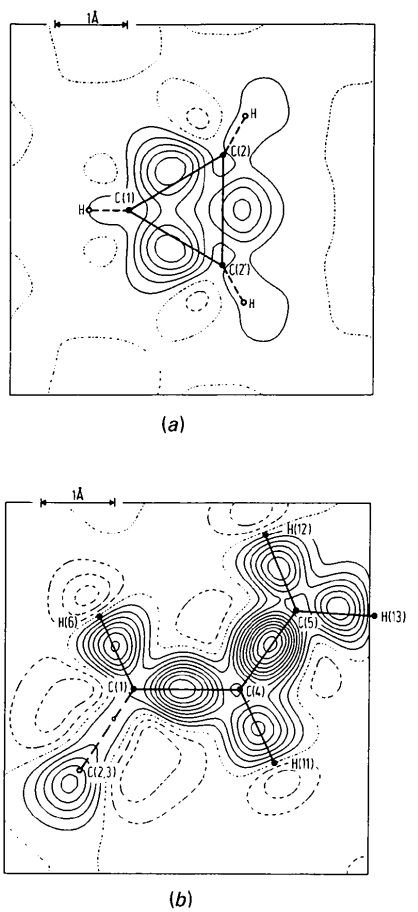

Fig. 2. DEF(model; **r**) maps showing unexpected deviations from pseudo-symmetry, see §2.7. (*a*) CP: ring plane, *S*(4,4) refinement. (*b*) VCP: C(1)C(4)C(5) plane, *S*(4,4)*E*,*A*3 refinement. Contours here and in the following figures, unless stated otherwise, are at intervals of 0·05 e Å^{-3}; full lines represent positive, dotted lines zero and dashed lines negative contours.

* Lists of structure factors for the three UM models have been deposited with the British Library Document Supply Centre as Supplementary Publication No. SUP 44634 (38 pp.). Copies may be obtained through The Executive Secretary, International Union of Crystallography, 5 Abbey Square, Chester CH1 2HU, England.

of the extension of the data set (for BCP and VCP with respect to CP), and the presence of an inversion centre (found only in BCP). According to Table 4 the correlation between ρ(IAM;**r**) and DEF(model;**r**) is small for BCP and VCP. Only CP, for which the extension of the data set into the high-order region is relatively small, has relevant C correlation coefficients $>0{\cdot}50$.

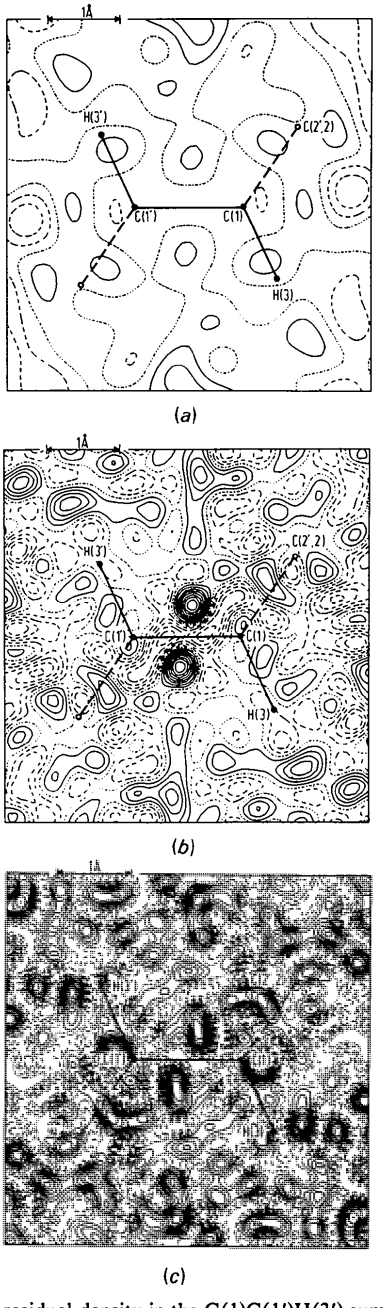

Fig. 3. BCP residual density in the C(1)C(1')H(3') symmetry plane for different resolutions $(\sin\theta)/\lambda$: (*a*) 0·65 Å^{-1}, (*b*) 1·00 Å^{-1}, (*c*) 1·20 Å^{-1}. Contour intervals are 0·01 e Å^{-3}.

Table 4. *Correlation coefficients $\rho(a,b)$ between IA parameter a and any other parameter b of the UM refinements*

For carbon $|\rho|$'s $> 0{\cdot}50$ and for hydrogen $|\rho|$'s $> 0{\cdot}65$ are listed. No relevant $|\rho|$'s have been found for VCP.

CP			BCP		
a	*b*	ρ	*a*	*b*	ρ
U_{23}[C(1)]	Pop(1,2,0)[C(1)]	−0·57	U_{22}[H(3)]	Pop(1,1,0)[H(3)]	−0·70
U_{23}[C(2)]	Pop(1,2,0)[C(2)]	−0·55	U_{13}[H(5)]	Pop(1,1,1+)[H(5)]	−0·68
Pop(1,0, 0)[C]	Pop(2,0,0)[C(1)]	−0·61			
U_{22}[H(3)]	Pop(2,0,0)[C(1)]	−0·75			
U_{33}[H(4)]	Pop(2,0,0)[C(1)]	−0·68			
U_{22}[H(3)]	Pop(2,0,0)[H]	0·75			
U_{33}[H(4)]	Pop(1,1,1−)[H(4)]	0·66			
U_{22}[H(5)]	Pop(1,1,0)[H(5)]	−0·69			

3. Dynamic filtered deformation density distributions

3.1. *Reliability of the multipole model*

Whether or not the UM models represent all systematic features available in the data must be decided on the basis of the residual density maps

$$\mathrm{DIF}(\mathbf{r}) = (\mathrm{Sc}_m)^{-1}[\rho_o(\mathrm{crystal};\mathbf{r}) - \rho(\mathrm{model};\mathbf{r})]. \quad (4)$$

For the centrosymmetric compound BCP, where model errors have the smallest chance of being masked by errors in the F_o phases, DIF(**r**) densities at the crystallographic mirror plane are given in Fig. 3 for resolutions $(\sin\theta)/\lambda = 0{\cdot}65$, 1·00 and 1·20 Å^{-1}. Standard deviations σ_{ar} at arbitrary positions estimated by the Cox & Cruickshank (1948) formula are $\sigma_{ar}(0{\cdot}65) = 7$, $\sigma_{ar}(1{\cdot}00) = 14$ and $\sigma_{ar}(1{\cdot}20) = 23 \times 10^{-3}$ e Å^{-3}. At special positions σ is estimated to increase by a factor of $\sqrt{2}$ for each symmetry element at the position considered. For regions not resolved from a symmetry element, part of the $\sqrt{2}$ factor has to be retained.

In view of the 0·65 Å^{-1} standard deviations which range from 10 to 14 e Å^{-3} for the BCP mirror plane, the 0·65 Å^{-1} map of Fig. 3(*a*) is flat within experimental error. Consequently, the multipole model gives an adequate description of the *low-resolution* features of the electron density distribution. For all three

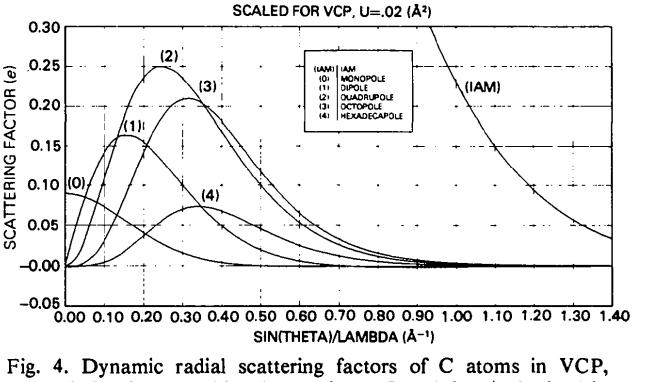

Fig. 4. Dynamic radial scattering factors of C atoms in VCP, multiplied for each *l* by the maximum $\mathrm{Pop}_\rho(i,l,m\pm)$ obtained in the $S(4,4)E$ refinement. $\langle u^2\rangle = 0{\cdot}02$ Å^2.

compounds the excellent fit of $|F_c|$ to $|F_o|$ for the low-order reflections is illustrated by the low R_w residuals for reflections up to $(\sin\theta)/\lambda = 0{\cdot}65$ Å^{-1}: 0·39% for CP, 0·57% for BCP and 0·32% for VCP.

In contrast with the 0·65 Å^{-1} map, the 1·00 Å^{-1} BCP map of Fig. 3(*b*) contains a significant peak of 0·088 (e.s.d. $\approx$0·025)e Å^{-3} at a distance of 0·4 Å from the 2/*m* position. However, in the 1·20 Å^{-1} map the peak is no longer significant or outstandingly high in comparison with other peaks. The presence of the significant peak in the 1·00 Å^{-1} map has been ascribed to series termination caused by high-resolution deficiencies in the multipole model, on the basis of the following arguments. According to Fig. 4, the contribution of the applied deformation functions to the intensities becomes negligible for $(\sin\theta)/\lambda > 1{\cdot}00$ Å^{-1}, indicating that the radial distribution functions do not show high-resolution features. Moreover, possible anharmonicities in the

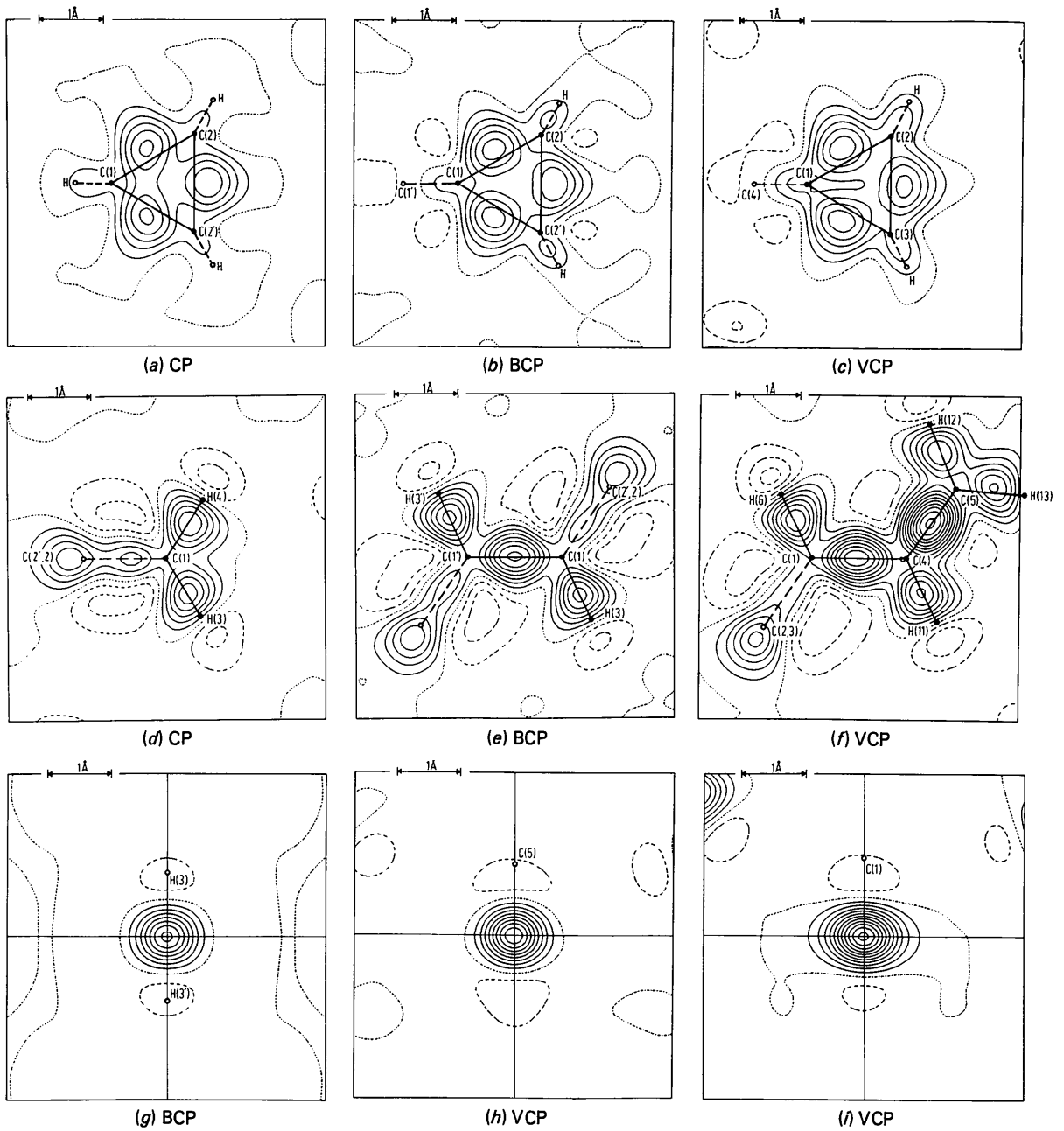

Fig. 5. Sections of $DEF_{exp}(\mathbf{r})$ maps. (*a*), (*b*), (*c*) Ring planes. (*d*) CP: C(1)H(4)H(3) plane. (*e*) BCP: C(1)C(1′)H(3′) plane. (*f*) VCP: C(1)C(4)C(5) plane. (*g*), (*h*), (*i*) Plane perpendicular to and through the midpoint of: (*g*) the BCP central bond, (*h*) the VCP central bond, and (*i*) the VCP double bond.

thermal vibrations have not been considered. For the map including reflections up to 1·20 Å^{-1} (close to the refinement limit) conceptual model errors will be balanced as much as possible by changes in the IA parameters $\mathbf{r}_p$ and $\mathbf{U}_p$. It is therefore not surprising that the 1·20 Å^{-1} map shows only random noise. Balancing is less complete, however, when the reflection set is limited to $(\sin\theta)/\lambda = 1{\cdot}00$ Å^{-1}. Especially for the 1·00 Å^{-1} DIF(**r**) map series-termination peaks due to model errors can thus be expected.

3.2 *Filtered deformation densities*

The deformation features extracted from the data by the multipole refinements are given [*cf.* (2)] by

$$\mathrm{DEF}_{\mathrm{exp}}(\mathbf{r}) \equiv \mathrm{DEF}(\mathrm{model};\mathbf{r}). \qquad (5)$$

As discussed above, $\mathrm{DEF}_{\mathrm{exp}}(\mathbf{r})$ only shows low-resolution deformations. Random errors in $\mathrm{DEF}_{\mathrm{exp}}(\mathbf{r})$ caused by the standard deviations in the deformation parameters are predominantly due to the $\sigma(F_o)$'s of the low-order reflections. For BCP, $\sigma_{\mathrm{ar}}(0{\cdot}65) = 0{\cdot}007$ e Å^{-3} is taken as a reasonable estimate for $\sigma_{\mathrm{ar}}[\mathrm{DEF}_{\mathrm{exp}}(\mathbf{r})]$, for regions $> 0{\cdot}4$ Å from the nuclei. Close to the nuclei the standard deviations will be higher owing to the influence of random errors in the IA parameters on DEF(model;**r**). For VCP with correlations (Table 4) and IA standard deviations comparable to BCP, the BCP $\sigma_{\mathrm{ar}}[\mathrm{DEF}_{\mathrm{exp}}(\mathbf{r})]$ value has also been accepted. For CP this σ_{ar} value is multiplied by a factor of two because of the larger correlation coefficients and IA standard deviations. Standard deviations at positions containing (pseudo-)symmetry elements are found by multiplying σ_{ar} by $\sqrt{2}$ for each available (pseudo-) symmetry element.

The $\mathrm{DEF}_{\mathrm{exp}}(\mathbf{r})$ maps of Fig. 5 and C—C bond peak heights listed in Table 2 are obtained by Fourier summation of the reflections up to $(\sin\theta)/\lambda = 1{\cdot}00$ Å^{-1}. The sections of the ring plane (Figs. 5*a,b,c*) clearly reveal the bent bond character of the ring C—C bonds. The sections perpendicular to and through the centre of the central bonds in BCP and VCP, and of the double bond in VCP show the expected deviation from a circular density distribution, which increases going from the 'single' bond in BCP *via* the 'single' bond in VCP to the double bond in VCP. A further discussion of the deformation densities will be given on the basis of the static deformation densities in paper III.

The computations were carried out at the Computing Centre of the University of Groningen. The investigations were supported in part by the Netherlands Foundation for Chemical Research (SON) with financial aid from the Netherlands Organization for the Advancement of Pure Research (ZWO).

References

BASTIANSEN, O., FRITSCH, F. N. & HEDBERG, K. (1964). *Acta Cryst.* **17**, 538–543.

BECKER, P. J. & COPPENS, P. (1974). *Acta Cryst.* A**30**, 129–147.

BENTLEY, J. & STEWART, R. F. (1976). *Acta Cryst.* A**32**, 910–914.

CLEMENTI, E. (1965). *Tables of Atomic Functions.* San José Research Laboratory, International Business Machines Corporation, San José, California, USA.

COX, E. G. & CRUICKSHANK, D. W. J. (1948). *Acta Cryst.* **1**, 92–93.

HAGEN, K., HAGEN, G. & TRÆTTEBERG, M. (1972). *Acta Chem. Scand.* **26**, 3649–3661.

HAMILTON, W. C. (1965). *Acta Cryst.* **18**, 502–510.

HEHRE, W. J., STEWART R. F. & POPLE, J. A. (1969). *J. Chem. Phys.* **51**, 2657–2664.

KEULEN, E. (1969). PhD Thesis. Univ. of Groningen, The Netherlands.

LEVIN, I. W. & PEARCE, R. A. R. (1978). *J. Chem. Phys.* **69**, 2196–2208.

NES, G. J. H. VAN & VAN BOLHUIS, F. (1979). *Acta Cryst.* B**35**, 2580–2593.

NIJVELDT, D. & VOS, A. (1988*a*). *Acta Cryst.* B**44**, 281–289.

NIJVELDT, D. & VOS, A. (1988*b*). *Acta Cryst.* B**44**, 296–307.

STEWART, R. F., BENTLEY, J. & GOODMAN, B. (1975). *J. Chem. Phys.* **63**, 3786–3793.

STEWART, R. F. & SPACKMAN, M. A. (1981). *VALRAY Users Manual.* Preliminary draft. Department of Chemistry, Carnegie–Mellon Univ., Pittsburgh, PA, USA.

TRÆTTEBERG, M. (1983). Private communication.

WAL, R. VAN DER (1982). PhD Thesis. Univ. of Groningen, The Netherlands.

Acta Cryst. (1988). B**44**, 296–307

Single-Crystal X-ray Geometries and Electron Density Distributions of Cyclopropane, Bicyclopropyl and Vinylcyclopropane. III. Evidence for Conjugation in Vinylcyclopropane and Bicyclopropyl

BY DICK NIJVELDT AND AAFJE VOS

Laboratory of Chemical Physics, University of Groningen, Nijenborgh 16, 9747 *AG Groningen, The Netherlands*

(*Received* 21 *November* 1986; *accepted* 9 *December* 1987)

Abstract

Starting from the qualitative Walsh model for cyclopropane (CP), a discussion is given on the influence of (possible) conjugation on the geometry and electron density distribution of bicyclopropyl (BCP) and vinylcyclopropane (VCP). Conjugation is expected to induce, for example, (i) geometric ring asymmetry and

0108-7681/88/030296-12$03.00